Identification of yellow rust in wheat using in-situ spectral reflectance measurements and airborne hyperspectral imaging

Wenjiang Huang · David W. Lamb · Zheng Niu · Yongjiang Zhang · Liangyun Liu · Jihua Wang

Abstract The aim of this study was to evaluate the accuracy of the spectro-optical, photochemical reflectance index (PRI) for quantifying the disease index (DI) of yellow rust (*Biotroph Puccinia striiformis*) in wheat (*Triticum aestivum L.*), and its applicability in the detection of the disease using hyperspectral imagery. Over two successive seasons, canopy reflectance spectra and disease index (DI) were measured five times during the growth of wheat plants (3 varieties) infected with varying amounts of yellow rust. Airborne hyperspectral images of the field site were also acquired in the second season. The PRI exhibited a significant, negative, linear, relationship with DI in the first season ($r^2 = 0.91$, $n = 64$), which was insensitive to both variety and stage of crop development from Zadoks stage 3–9. Application of the PRI regression equation to measured spectral data in the second season yielded a coefficient of determination of $r^2 = 0.97$ ($n = 80$). Application of the same PRI regression equation to airborne hyperspectral imagery in the second season also yielded a coefficient of determination of DI of $r^2 = 0.91$ ($n = 120$). The results show clearly the potential of PRI for quantifying yellow rust levels in winter wheat, and as the basis for developing a proximal, or airborne/spaceborne imaging sensor of yellow rust in fields of winter wheat.

W. Huang · Y. Zhang · L. Liu · J. Wang
State Key Laboratory of Remote Sensing Science, Jointly Sponsored by the Institute
of Remote Sensing Applications of Chinese Academy of Sciences and Beijing
Normal University, Beijing 100101, China

W. Huang · Z. Niu
National Engineering Research Center for Information Technology in Agriculture,
Beijing 100097, China

D. W. Lamb (✉)
Precision Agriculture Research Group, School of Science and Technology,
University of New England, Armidale, NSW 2351, Australia
e-mail: dlamb@une.edu.au

Introduction

Winter wheat (*Triticum aestivum L.*) is one of the most important crops in China. Yellow
rust (*Biotroph Puccinia striiformis*) is a fungal disease of this crop that produces leaf
lesions (pustules) that are yellow in color and tend to be grouped in patches. Yellow rust
often occurs in narrow stripes, 2–3 mm wide that run parallel to the leaf veins. Multiple
golden-yellow colored rust pustules, each the size of a pencil dot (≈ 200 µm $\times$ 150 µm)
are formed in the chlorotic areas. Yellow rust is responsible for approximately 73–85% of
recorded yield losses, and grain quality is also significantly reduced (Li et al. 1989).
Consequently, forecasting the incidence of this disease and the subsequent use of this
information to facilitate timely avoidance strategies are critical to enhancing the viability
of China's wheat production industry. Pesticides are a key management strategy. However,
excessive use of pesticides for plant disease treatment increases costs and raises the danger
of toxic residue levels in agricultural products. Disease control could be more efficient if
disease patches within fields could be identified and spray applied only to the infected
areas. Recent developments in optical sensor technology have the potential to enable direct
detection of foliar disease under field conditions (West et al. 2003).

The interaction of electromagnetic radiation with plants varies with the wavelength of
the radiation. The same plant leaves will exhibit significant differences in the way they
reflect light depending on the level of health and or vigor (Knippling 1970; Wooley 1971;
West et al. 2003). Healthy, vigorously growing plant leaves will generally have

(i)   low reflectance at visible wavelengths (400–700 nm) owing to strong absorption by
       photoactive pigments (chlorophylls, anthocyanins, carotenoids);
(ii)   high reflectance in the near infrared (700–1,200 nm) because of multiple scattering at
       the air-cell interfaces in the leaf's internal tissue; and
(iii) low reflectance in wide wavebands in the short-wave infrared (1,200–2,400 nm)
       because of absorption by water, proteins, and other carbon constituents.

Remote sensing of crop plant vigour has generally focused on the link between plant
pigments, especially chlorophylls, and biomass; the combination of which is collectively
referred to as photosynthetically active biomass-PAB (Hall et al. 2002). During the past
36 years there has been much literature generated on this type of work (for example
Knippling 1970; Thomas and Gausman 1977; Everitt et al. 1985; Bonham-Carter 1987;
Buschmann and Nagel 1993; Filella and Peñuelas 1994; Blackmer et al. 1996; Lamb et al.
2002, to name a few). Increasingly, developments in the remote sensing of agricultural
crops have been encouraged by the needs of precision agriculture. This is particularly so for
technologies that enable agricultural crops to be managed differentially on the basis of
spatial variation in predicted or actual yield and product quality (for example, Haboudane
et al. 2002; Huang et al. 2004), weed pressure (for example Lamb and Weedon 1998; Lamb
et al. 1999; Lamb and Brown 2001), crop nutrition (for example Thomas and Gausman
1977; Filella et al. 1995; Blackmer et al. 1996) and crop plant disease (for example
Lorenzen and Jensen 1989; Rinehart et al. 2002; West et al. 2003; Moshou et al. 2004).

Crop plant disease often influences transpiration rate, leaf color, morphology, and crop density therefore detection via remote sensing relies on the same pigment and biomass detection methods as for nutrient and yield. Many farmers worldwide currently rely on the visual sensing of optical changes in crop canopies as part of their day-to-day assessment of disease risk. However such assessments are time-consuming and can be inaccurate (Parker et al. 1995). The use of optical reflectance measurements and spectral indices appropriate for on-ground or overhead sensors offers several advantages over conventional visual appraisal methodologies. This includes the use of wavebands beyond the limit of human sensitivity, the ability to detect symptoms early (if pre-visual symptoms exist), and most importantly, the ability to co-analyze complex relationships between several properties.

Reflectance at 700 nm (red wavelength) and, more significantly, the ratio between reflectance at 700 nm and at 550 nm (green wavelength), is highly correlated with total leaf chlorophyll content (Gitelson et al. 1996). The use of near infrared (NIR) wavelengths (~750–2,500 nm) dates back to the 1930s when Bawden (1933) studied plant virus diseases by infrared photography. More recently, researchers have investigated the link between chlorophyll-related wavebands and crop plant diseases. For example, Sharp et al. (1985) researched the monitoring of cereal rust development with a spectral radiometer. Changes in leaf spectral properties induced in barley leaves by cereal powdery mildew were studied by Lorenzen et al. (1989). Hansen (1991) used multi-spectral radiometry to quantify yellow rust in wheat and Adams et al. (1999) introduced a yellowness index (YI) as a measure of chlorosis in leaves of stressed plants. Sasaki et al. (1999) were able to distinguish diseased cucumber leaves from healthy leaves at an early stage of infection, based upon the spectral reflectance of the leaves in the 500, 600, and 650 nm wavebands. In this work the disease classification error was only 10%. Rinehart (2002) investigated the relationship between canopy spectral reflectance and the severity of stripe patch and dollar spot (*Sclerotinia homeocarpa*) caused by diseases on creeping bentgrass. Moshou et al. (2004) studied the automatic detection of wheat yellow rust by in-situ reflectance measurements, and disease detection algorithms based on neural networks were developed. The research described above points clearly to the potential of spectral reflectance measurements for quantifying the incidence or severity of crop plant diseases, and some specifically related to rust in wheat. However, none of this research has evaluated the application of derived predictors of disease incidence to subsequent seasons, nor have they been applied to airborne hyperspectral remote sensing.

In this study, in-situ spectral reflectance measurements of crop plants infected with yellow rust were used to develop a regression equation to characterize the disease index. This was validated in the subsequent growing season, and then be applied to hyperspectral airborne imagery to discriminate and map the disease index in target fields.

Materials and methods

Experimental design and field conditions

The experiment was conducted at Beijing Xiaotangshan Precision Agriculture Experimental Base, in Changping district, Beijing (40°10.6′ N, 116°26.3′ E) for the 2001–2002 and 2002–2003 growing seasons. Experimental data from 2001 to 2002 were used to establish the statistical models, and the data for 2002–2003 were used to validate the models developed.

The field site has a warm temperate climate, with a mean annual rainfall of 507.7 mm and a mean annual temperate of 13°C. In this region a significant proportion of growing days are cloudless during April to June. The soil at the sites is a silt-clay loam. The average topsoil nutrient status (0–0.30 m depth) was as follows: organic matter 1.42–1.48%, total nitrogen 0.08–0.10%, alkali-hydrolysis nitrogen 58.6–68.0 mg kg^{-1}, available phosphorus 20.1–55.4 mg kg^{-1}, and rapidly available potassium 117.6–129.1 mg kg^{-1}.

The crop at the field site was winter wheat (*Triticum aestivum L.*) and three cultivars of wheat were planted; 'Jing 411' on 2.4 ha, '98–100' on 1.2 ha and 'Xuezao' on 1.2 ha. Jing 411 has a strong resistance to yellow rust, 98–100 has moderate resistance and Xuezao is susceptible to it.

Inoculation and assessment of disease index

Yellow rust (*Biotroph Puccinia striiformis*) was inoculated by spore inoculation according to the National Plant Protection Standard (Li et al. 1989) on April 1 2002 and April 4 2003, both times coincide with the 'erecting' stage of plant development (approximately Zadoks stage 25) (Zadoks et al. 1974). A visual inspection of disease severity was done at 5–7 day intervals following inoculation with exact intervals selected to include stem elongation (Zadoks stage 3), heading, anthesis (Zadoks stage 5), grain filling (Zadoks stage 7), milky maturity (Zadoks stage 8) and wax ripeness (Zadoks stage 9) stages of plant development. Disease severity was determined as the proportion of a complete leaf covered by yellow rust spores. On each inspection, the plants were grouped into one of 9 classifications of disease incidence (x); 0, 1, 10, 20, 30, 45, 60, 80 and 100% covered by rust. Zero percent represented no incidence of yellow rust and 100% was the greatest incidence. The disease index (DI) was then calculated using (Li et al.1989):

$$
\mathrm{DI} = \frac{\sum\limits_{n=0}^{8} (x \times f)}{n \times \sum\limits_{n=0}^{8} f} \times 100 \qquad (1)
$$

where f is the total number of leaves of each degree of disease severity and n is the highest degree of disease severity observed (in this work, $n = 8$).

Spectral reflectance measurements

In-situ canopy spectral reflectance measurements were acquired at the same time as the inspections for DI were carried out. Spectral reflectance measurements were recorded at a height of 1.6 m above ground by an ASD FieldSpec Pro spectrometer (Analytical Spectral Devices, Boulder, CO, USA) fitted with a 25° field of view fore-optic. Spectra were acquired in the 350–2,500 nm spectral region with a sampling interval of 1.4 nm between 350 nm and 1,050 nm, and 2 nm between 1,050 nm and 2,500 nm. Measured irradiance was converted into reflectance by recording irradiance spectra also from a 0.4 m × 0.4 m BaSO$_4$ calibration panel. All irradiance measurements were recorded as an average of 20 individual measurements (minus dark current) at an optimized integration time. All measurements were made under clear blue sky conditions between 10:00 h and 14:00 h (Beijing Local Time).

Airborne hyperspectral imaging

Airborne hyperspectral images of the trial field were acquired in 2003 using the Pushbroom Hyperspectral Imager (PHI) (Shao 1998) designed by the Chinese Academy of Science (CAS) and flown onboard a Yun-5 aircraft (Shijiazhuang Aircraft Manufacturing Company, China). The PHI comprises a solid state, area array, silicon CCD device of 780×244 elements, has a field of view of $21°$ and is capable of acquiring images of $1\,m \times 1\,m$ spatial resolution at an altitude of 1,000 m above ground. It has a wavelength range of 400–850 nm with a spectral resolution of 5 nm. Images of the target field were acquired in 2003 at the phenological growth stages of stem elongation (April 18, 2003, Zadoks stage 3), anthesis (May 17, 2003, Zadoks stage 5) and milky maturity (May 31, 2003, Zadoks stage 8). The inoculated wheat was adequately infected by rust on April 18, obviously infected by May 17, and seriously infected by May 31. Measurements of DI were made and in-situ canopy reflectance spectra were also acquired on the same dates. All images were geometrically and radiometrically corrected using an array of georeferenced light and dark targets ($5\,m \times 5\,m$) located at the extremes of the field site. The aforementioned field spectrometer was used to calibrate these targets relative to $BaSO_4$. The location of each target, as well as any field measurements of DI were recorded using a differential global positioning system (Trimble Sunnyvale California, USA). A full summary of field activities is given in Table 1.

Photochemical reflectance index (PRI)

Since foliar pigments are destroyed and foliar physiological activity decreases following inoculation by the yellow rust epiphyte, the photochemical reflectance index (PRI) (Peñuelas et al. 1995) was selected as the spectrophotometric method of estimating the disease index. The PRI was calculated from the acquired reflectance spectra (R) by (Peñuelas et al. 1995)

$$\mathrm{PRI} = \left(\frac{(R_{531} - R_{570})}{(R_{531} + R_{570})}\right) \tag{2}$$

where, R_x corresponds to the reflectance at specific annotated wavelengths.

Results

The two consecutive growing seasons covered by this study had similar temperatures and rainfall patterns. Yield ranges for both healthy and rust-affected wheat were also similar, as

Table 1 Summary of field measurement activities for 2001–2002 and 2002–2003

Activity	2001–2002	2002–2003
Planting date	September 28	September 30
Inoculation of Rust	April 1	April 4
DI measurements	5–7 day intervals (Z3–Z9)	5–7 day intervals (Z3–Z9)
Spectral reflectance measurements	Coincident with DI measurements	Coincident with DI measurements
PHI images acquired	–	April 18, May 17, May 31

was the grain protein content. A summary of conditions and yield and quality ranges is given in Table 2.

PRI versus DI

A plot of the measured DI as a function of PRI for all varieties combined in 2001–2002 is given in Fig. 1. The data points associated with the variety Xuezao dominate the top left-hand region of the scatter plot (relatively high range of DI), those associated with the variety 98–100 are located in the mid region (mid-range DI) and those associated with Jing 411 dominate the lower-right region. This distribution is consistent with the relative susceptibility of these varieties to rust—Xuezao being the least resistant and Jing 411 having the greatest resistance. The regression equation of DI using PRI in 2001–2002 was observed to have the form ($n = 64$)

$$\mathrm{DI}(\%) = -721.22(\mathrm{PRI}) + 2.40 \left(-0.14 \le \mathrm{PRI} \le 0.02; r^2 = 0.91\right) \tag{3}$$

An important feature of Fig. 1, and the associated regression equation (Eq. 3), is that the spectrally-derived PRI explains 91% of the variance observed in the disease index. This explanation also encompasses the three varieties of wheat as well as the four stages of crop development for each variety. This is shown in Fig. 2 where the data from each variety are plotted individually with growth stage indicated, and the regression line (Eq 3) is also included. It is evident that the development stage of the varieties does not confound the discrimination of rust incidence. The displacement of the data along the calibration line, with increasing crop maturity, is the result of an increase in rust incidence only.

In the subsequent validation of the PRI–DI regression equation with the 2002–2003 data (Fig. 3), the coefficient of determination (r^2) between the estimated and measured values was 0.97 ($n = 80$).

In Fig. 3, the locations of data points associated with individual varieties are consistent with the levels of resistance to rust; Xuezao dominates the top right-hand region of the scatter plot (relatively high range of DI), the variety 98–100 has points scattered all along the regression line (predominantly mid-range DI) and Jing 411 is concentrated in the central lower-left region (lower range DI). The distribution of the individual development stages for each variety was again consistent with that observed for the previous season in Fig. 2 (data for 2003 not shown).

Application of multi-temporal PHI images for DI estimation

The DI was estimated, on a pixel-by-pixel basis, in each of the acquired PHI images using Eqs. 2 and 3. To map the degree of yellow rust infection in the trial field, the DI

Table 2 Summary of climate, crop yield and grain quality in 2001–2002 and 2002–2003 seasons

Activity	2001–2002	2002–2003
Rainfall (planting–harvest)	261.4 mm	228.9 mm
Yield range (healthy wheat, low–high vigour)	6,300–7,650 kg ha^{-1}	6,200–7,320 kg ha^{-1}
Yield range (infected wheat, DI = 100–10%)	750–6,000 kg ha^{-1}	600–6,300 kg ha^{-1}
Grain protein range (%) (healthy wheat)	15.1–16.7	15.4–16.8
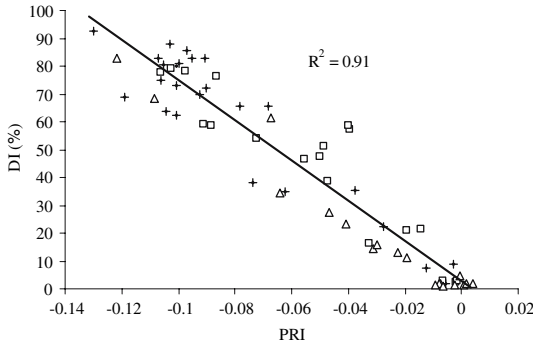
Fig. 1 Plot of measured disease index (DI) as a function of measured photochemical reflectance index (PRI) for all varieties combined in 2001–2; 'Δ' = Jing 411; '+' = Xuezao; '□' = 98–100

Fig. 2 Plots of measured disease index (DI) as a function of measured photochemical reflectance index (PRI) for individual varieties highlighting the location of data from each development stage (Zadok stage 3–9) in 2001–2002. Solid line is the PRI regression line from Eq. 3
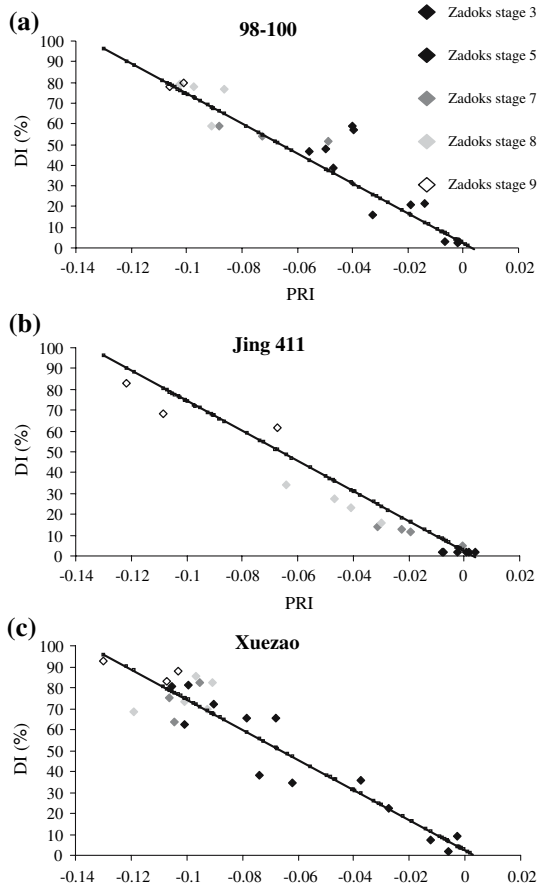
Fig. 3 Comparison of measured
DI and PRI-estimated DI for
2002–3; '∆' = Jing 411;
'+' = Xuezao; '□' = 98–100
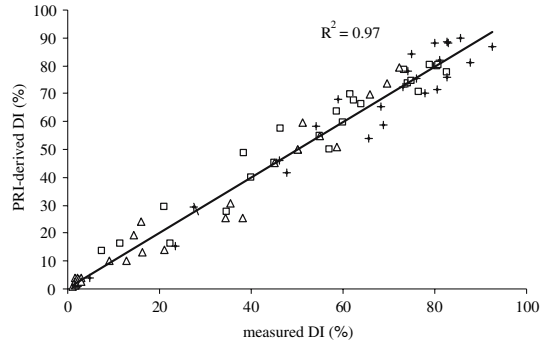
was binned into the following classes; Very Serious (DI > 80%), Serious (45% < DI ≤ 80%), Mid-range (10% < DI ≤ 45%), Low-range (1% < DI ≤ 10%) and None (0 < DI ≤ 1%). Classified images of the trial site comprising the three varieties (98–100 top left quadrant, Xuezao bottom left quadrant and Jing 411 right half of field), color-coded according to the 5 disease classes are given in Fig. 4. Early in the season (Stem elongation, Zadoks stage 3, April 18 2003) the more susceptible variety Xuezao appears to be performing better than the other two, although this is an artifact of higher biomass levels (tiller numbers) rather than reduced disease incidence. As the growing season progresses through anthesis (May 17, 2003, Zadoks stage 5) and milky maturity (May 31, 2003, Zadoks stage 8) the rust develops extensively throughout Xuezao in comparison to the other two varieties. This can be seen by the large values of DI for the south western quadrant of the field.

The relationship between the DI calculated from the multi-temporal PHI images and the actual measured DI from the 120 sample sites located within the field is given in Fig. 5. The coefficient of determination between the PHI—derived estimates of DI and actual DI is 0.91 ($n = 120$).
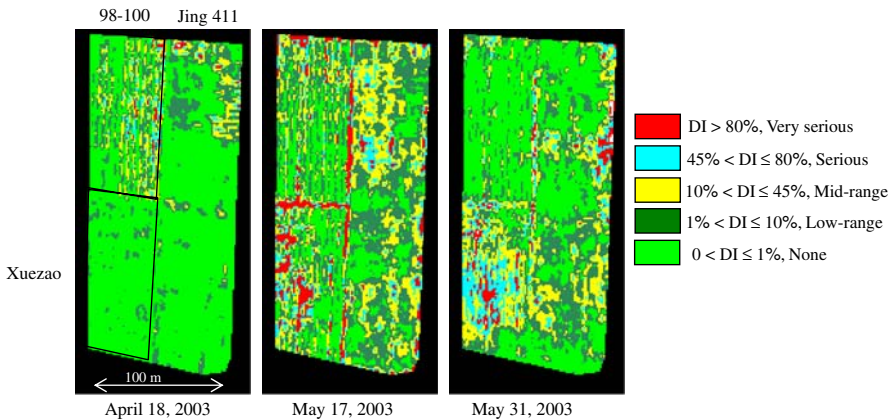
Fig. 4 Classified DI images derived from PHI airborne images of the trial site in 2003. Location of cultivars as indicated

Fig. 5 Comparison of PHI-derived estimates of DI and actual DI values for 2002–2003. Data were extracted from all three imaging times, although the DI values were < 20% for the April 18 image
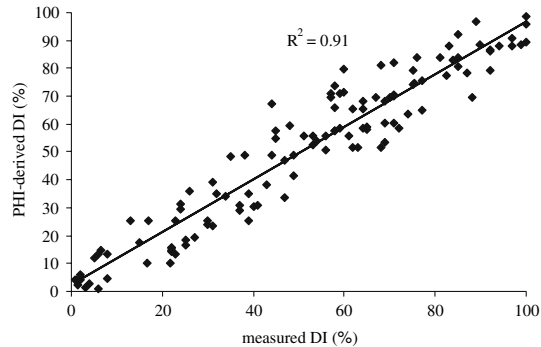
Discussion and conclusion

The level of variance explained in the calibration regression equation (Eq. 3) and the large coefficients of determination resulting from the subsequent validation measurements (both from spectroscopy and hyperspectral imagery) are encouraging given that the spatial variation in factors such as biomass and foliar nitrogen content would also be expected to influence PRI (Peñuelas et al. 1995). Given that PRI is expected to be positively correlated to biomass and foliar nitrogen content (Aparicio et al. 2000; Trotter et al. 2002) and rust incidence is generally negatively correlated (for example Neumann et al. 2004), it is not surprising that PRI is observed to be a robust spectral index in quantifying yellow rust infection.

This study was done for a single field site and spectral reflectance characteristics of crop plants are a function of a broad range of environmental factors that include soil type and texture, nutrient and water status, variety, stage of development and seasonal effects. Therefore, in spite of the comments in the paragraph above, future work should include such environmental parameters to validate further the relations observed in this study. Nevertheless, the results of this work confirm PRI is a potential candidate for operational use in the monitoring of yellow rust, and could form the basis of an on-the-go sensor and variable-rate spray applicator or a remote detection and mapping process.

References

Adams, M. L., Philpot, W. D., & Norvell, W. A. (1999). Yellowness index: An application of spectral second derivatives to estimate chlorosis of leaves in stressed vegetation. *International Journal of Remote Sensing, 20*, 3663–3675.

Aparicio, N., Villegas, D., Casadesus, J., Araus, J. L., & Royo, C. (2000). Spectral vegetation indices as nondestructive tools for determining durum wheat yield. *Agronomy Journal, 92*, 83–91.

Bawden, F. C. (1933). Infrared photography and plant virus diseases. *Nature, 132*, 168.

Blackmer, T. M., Schepers, J. S., Varvel, G. E., & Walter-Shea, E. A. (1996). Nitrogen deficiency detection using reflected shortwave radiation from irrigated corn canopies. *Agronomy Journal, 88*, 1–5.

Bonham-Carter, G. F. (1987). Numerical procedures and computer program for fitting an inverted Gaussian model to vegetation reflectance data. *Computers and Geosciences, 14*, 339–356.

Buschmann, C., & Nagel, E. (1993). In vivo spectroscopy and internal optics of leaves as basis for remote sensing of vegetation. *International Journal of Remote Sensing, 14*, 711–722.

Everitt, J. H., Richardsen, A. J., & Gausman, H. W. (1985). Leaf reflectance-chlorophyll relations in buffelgrass. *Photogrammetric Engineering and Remote Sensing, 51*, 463–466.

Filella, I., & Peñuelas, J. (1994). The red-edge position and shape as indicators of plant chlorophyll content, biomass and hydric status. *International Journal of Remote Sensing, 15*, 1459–1470.

Filella, I., Serrano, L., Serra, J., & Peñuelas, J. (1995). Evaluating wheat nitrogen status with canopy reflectance indices and discriminant analysis. *Crop Science, 35*, 1400–1405.

Gitelson, A. A., & Merzlyak, M. N. (1996). Signature analysis of leaf reflectance spectra: algorithm development for remote sensing of chlorophyll. *Journal of plant physiology, 148*, 494–500.

Haboudane, D., Miller, J. R., Tremblay, N., Zarco-Tejada, P. J., & Dextraze, L. (2002). Integrated narrow-band vegetation indices for prediction of crop chlorophyll concentration for application to precision agriculture. *Remote Sensing of Environment, 81*, 416–426.

Hall, A., Lamb, D. W., Holzapfel, B., & Louis, J. (2002). Optical remote sensing applications for viticulture—a review. *Australian Journal of Grape & Wine Research, 8*, 36–47.

Hansen, J. G. (1991). Use of multispectral radiometry in wheat yellow rust experiments. *OEPP/EPPO Bulletin, 21*, 651–658.

Huang, W. J., Wang, J. H., Wang, Z. J., Zhao, C. J., & Wang, J. D. (2004). Inversion of foliar biochemical parameters at various physiological stages and grain quality indicators of winter wheat with canopy reflectance. *International Journal of Remote Sensing, 25*, 2409–2419.

Knippling, E. B. (1970). Physical and physiological basis for differences in reflectance of visible and near-infrared radiation from vegetation. *Remote Sensing of Environment, 1*, 155–159.

Lamb, D. W., & Brown, R. B. (2001). Remote sensing and mapping of weeds in crops. *Journal of Agriculture Engineering Research, 78*, 117–125.

Lamb, D. W., & Weedon, M. (1998). Evaluating the accuracy of mapping weeds in fallow fields using airborne digital imaging. Panicum effusum in oilseed rape stubble *Weed Research, 38*, 443–451.

Lamb, D. W., Weedon, M. M., & Rew, L. J. (1999). Evaluating the accuracy of mapping weeds in seedling crops using airborne digital imaging. *Avena* spp. in seedling triticale (X *Triticosecale*). *Weed Research, 39*, 481–492.

Lamb, D. W., Steyn-Ross, M., Schaare, P., Hanna, M., Silvester, W., & Steyn-Ross, A. (2002). Estimating leaf nitrogen concentration in ryegrass (Lolium spp.) pasture using the chlorophyll red-edge: Theoretical modeling and experimental observations. *International Journal of Remote Sensing, 23*, 3619–3648.

Li, G. B., Zeng, S. M., & Li, Z. Q. (1989). *Integrated Management of Wheat Pests* (pp. 185–186). Beijing: *Press of Agriculture Science and Technology of China* (in Chinese).

Lorenzen, B., & Jensen, A. (1989). Changes in leaf spectral properties induced in barley by cereal powdery mildew. *Remote Sensing of Environment, 27*, 201–209.

Moshou, D., Bravo, C., West, J., Wahlen, S., McCartney, A., & Ramon, H. (2004). The automatic detection of 'yellow rust' in wheat using reflectance measurements and neural networks. *Computers and Electronics in Agriculture, 44*, 173–188.

Neumann, S., Paveley, N. D., Beed, F. D., & Sylvester-Bradley, R. (2004). Nitrogen per unit leaf area affects the upper asymptote of *puccinia striiformis* f.sp. *tritici* epidemics in winter wheat. *Plant Pathology, 53*, 725–732.

Parker, S. P., Shaw, M. W., & Royle, D. J. (1995). The reliability of visual estimates of disease severity on cereal leaves. *Plant Pathology, 44*, 856–864.

Peñuelas, J., Filella, I., & Gamon, J. A. (1995). Assessment of photosynthetic radiation use efficiency with spectral reflectance. *New Phytologist, 131*, 291–296.

Rinehart, G. L., Cathoun, J. H., & Schabbenberger, O. (2002). Remote Sensing of Stripe Patch and Dollar Spot on creeping Bentgrass and Annual Bluegrass Turf Using Visible and Near-infrared Spectroscopy, Australian Turfgrass Management Volume 4.2.

Sasaki, Y., Okamoto, T., Imou, K., & Torii, T. (1999). Generating of Distinction Parameter for Automatic Diagnosis of Plant Disease by GP. *Journal of the Japanese Society of Agricultural Machinery, 61*, 73–80 (in Japanese).

Shao, H., Wang, J. Y., & Xue, Y. Q. (1998). Key technology of pushbroom hyperspectral imager (PHI). *Journal of Remote Sensing, 2*, 251–255 (in Chinese).

Sharp, E. L., Perry, C. R., Scharen, A. L., Boatwright, G. O., Sands, D. C., Lautenschlager, L. F., Yahyaoui, C. M., & Ravet, F. W. (1985). Monitoring cereal rust development with a spectral radiometer. *Phytopathology, 75*(8), 936–939

Thomas, J. R., & Gausman, H. W. (1977). Leaf reflectance vs. leaf chlorophyll and carotenoid concentrations for eight crops. *Agronomy Journal, 69*, 799–802.

Trotter, G. M., Whitehead, D., & Pinkney, E. J. (2002). The photochemical reflectance index as a measure of photosynthetic light use efficiency for plants of varying foliar nitrogen contents. *International Journal of Remote Sensing, 23*, 1207–1212.

West, J. S., Bravo, C., Oberti, R., Lemaire, D., Moshou, D., & McCartney, H. A. (2003). The potential of optical canopy measurement for targeted control of field crop disease. *Annual Reviews of Phytopathology, 41*, 593–614.

Wooley, J. T. (1971). Reflectance and transmittance of light by leaves. *Plant Physiology, 47*, 656–662.

Zadoks, J. C., Chang, T. T., & Konzak, C. F. (1974). A decimal code for the growth stages of cereals. *Weed Research, 14*, 415–421.